STRESS CONCENTRATION FACTORS IN SPHERICAL VESSELS WITH SINGLE OBLIQUE NOZZLE

K. Naderan-Tahan

Department of Mechanical Engineering
Shahid Chamran University
Ahwaz, Iran

Abstract Finite element method is employed to analyze the spherical vessel intersected by an oblique cylindrical nozzle. In this survey the stress and strain distributions on acute and obtuse sides of the connection under internal pressure are studied widely although axial and moment loadings on the nozzle are also studied briefly. Stress concentration factors for a wide range of geometrical ratios in term of membrane stress in the sphere are calculated and presented. Variation of these factors with angle of obliquity of the branch is also investigated. The results are compared with measured quantities and with those mentioned in other references. It is assumed that the definition of thin shell is valid for both vessel and nozzle simultaneously and that the corners are sharp without any reinforcement. ABAQUS computer program is used in this survey.

Kew Words ABAQUS, Axial Load, Bending Moment, Cylindrical, Equivalent Radius, Finite Element Method, Membrane, Non-radial, Nozzle, Oblique, Spherical, Thin Shell, Vessel

چکیده سازه‌ای که از اتصال یک استوانه‌ای به یک کره بصورت غیر شعاعی حاصل می‌شود، یک سازه نامتقارن است و روش المان معین بعنوان یکی از روشهای آنالیز این سازه، مورد استفاده قرار گرفته است. در این بررسی، توزیع تنش‌ها و تغییر شکل‌های نسبی در دوطرف حاده و منفرجه انشعاب مایل تحت تأثیر فشار داخلی و بارهای متمرکز محوری و ممان خمشی، مورد مطالعه قرار گرفته است و سپس ضرائب تمرکز تنش برای پارامترهای هندسی مختلف بر حسب تنش غشایی مخزن کروی هم در مخزن و هم در انشعاب محاسبه شده و بصورت جدول و نمودار ارائه گردیده‌اند. تغییرات این ضرائب با زاویه تمایل انشعاب نیز نشان داده شده است. در مواردی که امکان داشته است نتایج حاصل با نتایجی که از آزمایش حاصل شده‌اند و در منابع دیگر وجود دارند مقایسه شده‌اند. فرض شده است که مخازن و اتصال از پوسته نازک ساخته شده باشند و گوشه‌ها در محل اتصال تیز و بدون مواد تقویت کننده باشد. برای آنالیز این سازه از برنامه کامپیوتری المان معین آباکوس استفاده شده است.

INTRODUCTION

Due to lack of analytical data, experimental results and relations are used in Codes and standards, [1,2] to design spherical vessels with oblique nozzles which is in contradiction to the "Design by analysis" philosophy of these vessels. Naderan-Tahan [3] analyzed this structure directly by the use of finite element method. The concept of "equivalent radius" for oblique nozzles to determine the stress concentration factors using the results obtained from the analysis of a radial nozzle is presented in [4]. Although shallow shell theory is the main restriction of this method, its theoretical results are, in some cases, consistent with the experimental findings. Effort is made to analyze the oblique connections to spherical vessels under external loadings in [5] but the restrictions imposed on geometrical ratios and small angles of obliquity are so severe that its application as a general method is limited. To reduce these restrictions, another analytical method is presented in [6]. The application of this method is

more general but the assumption of plane curve of the junction still imposes considerable restrictions. Using this method, a protruding nozzle is studied in [7]. Oblique connections to spherical shells under internal pressure and external loadings are studied in [8]. The method presented in [6] and [7] are used and the stress fields in such connections are compared with a single radial nozzle. The theoretical results are also compared with the experimental results obtained from testing steel models equipped with strain gauges and the agreement of the results is confirmed for specified angles of obliquity. Reference [9] contains stress data obtained in photoelastic method for oblique connections and large angles of obliquity are also investigated. The state of the art and summary of the existing data related to the design of oblique nozzles to spherical vessels are explained in [10]. The performance and the validity of the finite element method and computer program ABAQUS [11] to analyze such structures is investigated in [12]. In this reference a radial nozzle is considered as a limiting case of oblique nozzle with zero anlge of obliquity and the application of this program to analyze oblique connection to sphere is recommended.

METHOD OF ANALYSIS

The use of general shell element of a finite element computer program provides a tool to analyze the spherical vessel intersected by an oblique cylinder which is a nonsymmetrical structure. The performance of such element and the ABAQUS computer program are studied already in [12]. The application of this kind of element to analyze radial connections as a limiting case of oblique nozzle with zero angle of obliquity has strengthened the idea to use it for other than zero angles. It is tried to apply finite element method as a simple and reliable method for direct analysis of such structures under internal pressure and external loadings with any anlge of obliquity.

Finite element model

The vessel is considered as a hemisphere having a nonradial connection at angles 22.5° and 45°. Since there is a plane of symmetry, a finite element model is prepared for half of the vessel by dividing the junction curve into ten parts. Each part is used as a side of general shell element with eight nodes to produce a suitable mesh on both sphere and cylinder. Care is taken to lay the sides of elements along the circles and meridians in order to avoid element distortion specially for large angle of obliquity. Suitable boundary conditions are imposed to provide continuity of displacement and rotation of common nodes at 21 points of the junction curve and a mesh adequately fine was produced. The flush connection is considered to have sharp edges and it is assumed that the thin shell definition is valid simultaneously in vessel and nozzle. Figure 1 illustrates a finite element model of the structure in which the angle of obliquity is 22.5°.

The angle of obliquity α is defined as the anlge between the axis of the nozzle and the radius of the

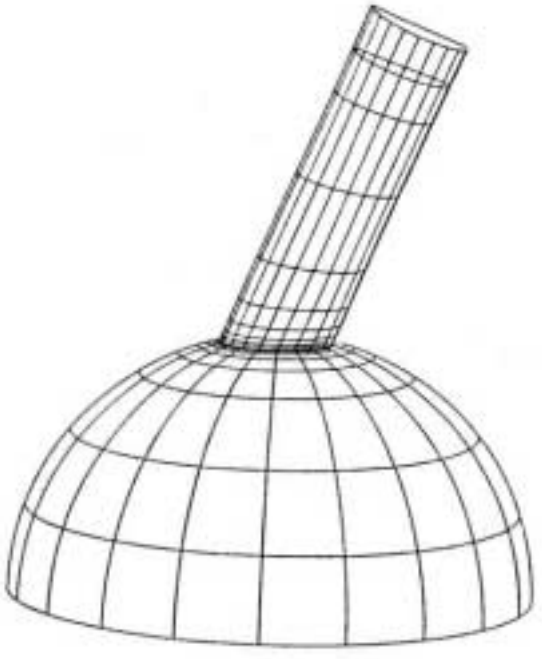

Figure 1. Finite element mesh of model 1

vessel at the intersection point. The range of geometrical parameters of structure considered in this study are: $625 \geq R/T \geq 10$, $0.5 \geq r/R \geq 0.05$, $1.0 \geq t/T \geq 0.25$, where R, T, r, and t are the radius and thickness of vessel and connection respectively.

Two models were prepared in order to investigate the stress fields around the junction and obtain a better understanding of stress concentration factors. The specifications of these models are as follows:

	α	R,mm	T,mm	r,mm	t,mm	E,Mpa	ν
Model 1	22.5°	68.71	1.91	11.65	0.95	7×10^4	0.32
Model 2	45°	50	1	10	1	20×10^4	0.30

E is the modulus of elasticity and ν is the Poisson's ratio.

The specifications of the model 1 are selected from an aluminium test model in order to make the comparison between theoretical and experimental data possible.

The stress distributions along the generators in the plane of symmetry for both obtuse and acute sides of the vessel and the effect of obiliquity angle on the stress concentration factors are studied first. The extent of decay length and the stress contours on the inside and outside surface of the vessel were also investigated. The total number of models analyzed were 85. In 51 models α was kept constant at 22.5° and in 34 models it was 45°. Total number of elements on half of the vessel is 180 with 605 nodes and 3630 degrees of freedom. The approximate CPU time to run the program on Cyber 205 super computer was 130 second for elastic analysis of each model.

RESULTS

A sample of stress distributions in spherical vessel and its oblique connection is shown in Figure 2. The parameter used for calculating dimensionless stresses is PR/(2T) which is the membrane stress in the vessel, in which P is internal pressure. In this figure the hoop and meridional stresses on the inside and outside surfaces of vessels for which $\alpha = 22.5°$ and 45° are plotted. Shear stresses along the junction curve when α is 22.5° are also indicated. As it is clear from these diagrams the maximum stresses appeare at the acute side of the connection for which $\theta = 180°$ (θ is a spherical coordinate measured according to the right hand rule from the plane of symmetry, $\theta = 0°$ is used for obtuse side and $\theta = 180°$ for acute side of the vessel). Changes in stresses are very severe in this region. In further studies it was revealed that the maximum stresses and the maximum stress concentration factors appear in connection as far as $t/T \leq 1$.

The Stress Concentration Factors (SCF) using maximum shear stress τ_{max}, i.e. $SCF = 2\tau_{max}/(PR/2T)$ are listed in Tables 1 and 3. Maximum principal stress σ_1 is used to prepare Tables 2 and 4.

The variation of these factors with dimensionless parameter $\sqrt{(R/T)}$ and for various t/T values are plotted in Figure 3.

Table 5 indicates the variation of SCF values with the angle of obliquity and a corresponding diagram is presented in Figure 4. The data for zero angle of obliquity (radial nozzle) are taken from [12].

SCF values obtained by FEM are compared with those obtained by "Equivalent radius" method in table 6. An equivalent radius $r' = r Sec\alpha$ is calculated according to this method. By entering this value into the corresponding curves for radial connection, and multiplying the corresponding SCF by *Seca*, the stress concentration factors for the oblique nozzle of radius r at angle α are determined. From this table it is clear that the former values are always greater than the latter ones. In this table ρ is a dimensionless parameter defined as $\rho = (r/R)\sqrt{(R/T)}$.

Other types of loading

Distribution of hoop and meridional stresses in a

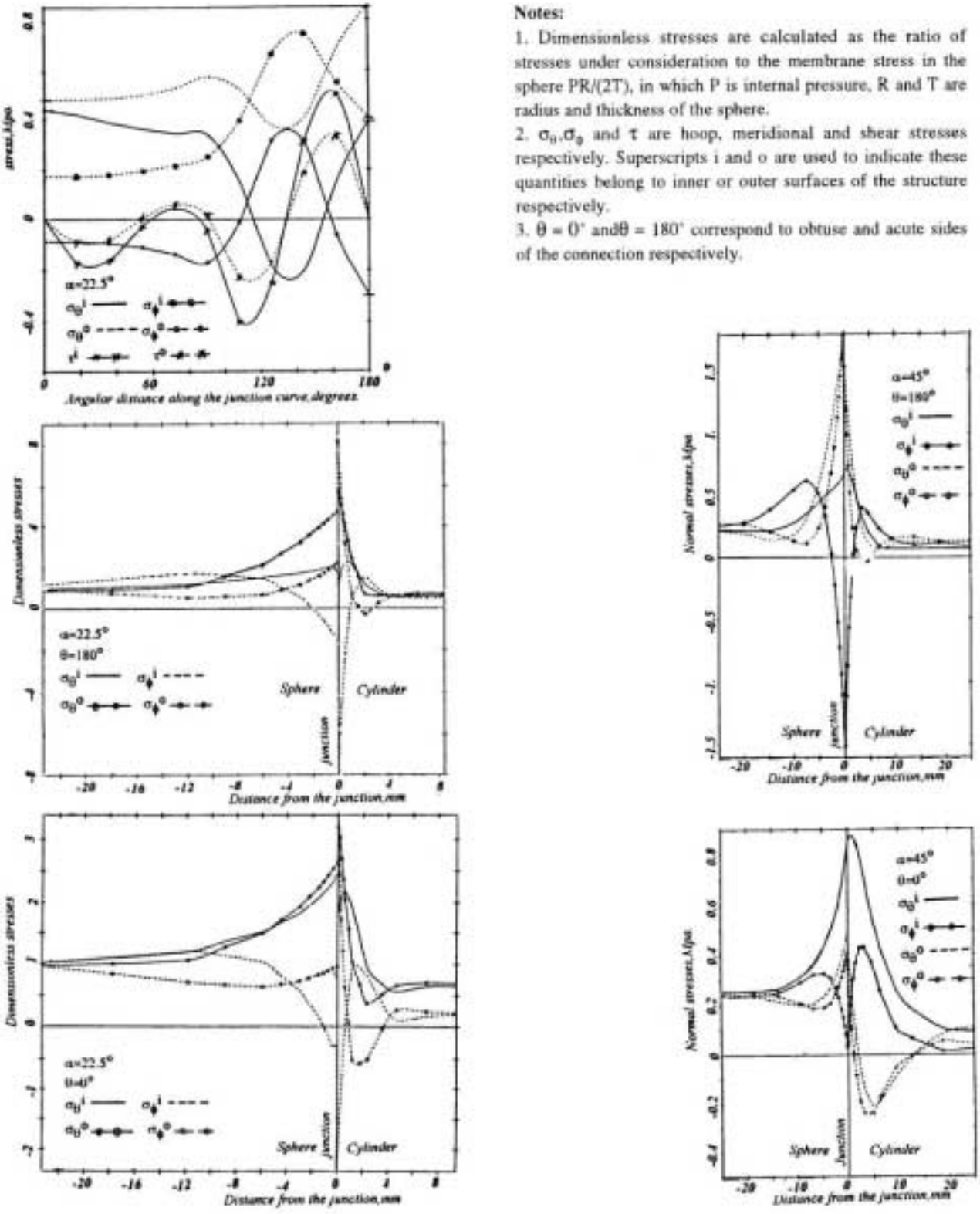

Notes:

1. Dimensionless stresses are calculated as the ratio of stresses under consideration to the membrane stress in the sphere PR/(2T), in which P is internal pressure, R and T are radius and thickness of the sphere.
2. $\sigma_\theta, \sigma_\phi$ and τ are hoop, meridional and shear stresses respectively. Superscripts i and o are used to indicate these quantities belong to inner or outer surfaces of the structure respectively.
3. $\theta = 0^\circ$ and $\theta = 180^\circ$ correspond to obtuse and acute sides of the connection respectively.

Figure 2. Stress distributions on the inner and outer surfaces of the Model 1 (left) and Model 2 (right) under internal pressure P=0.01 Mpa.

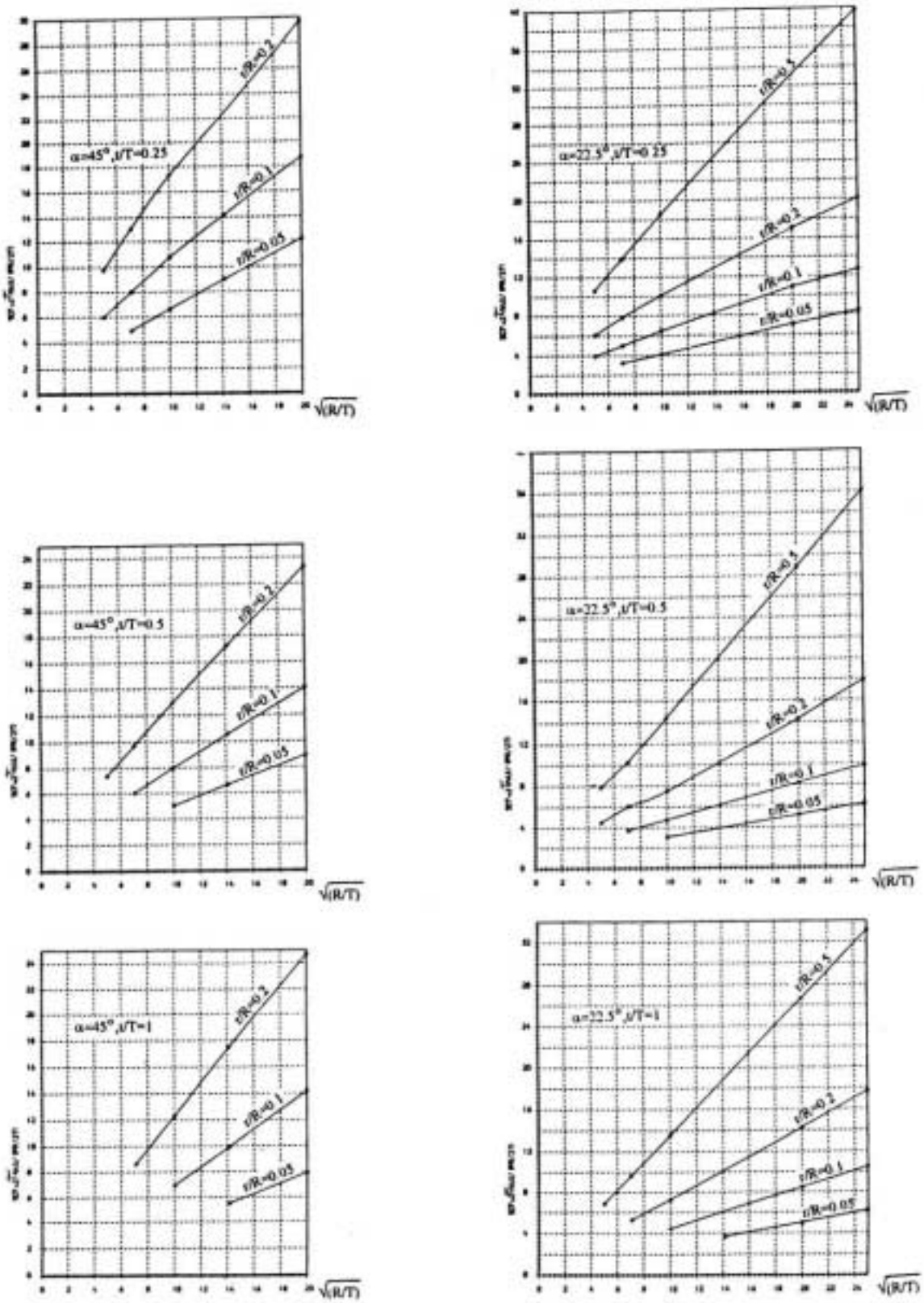

Figure 3. Diagrams of Stress Concentration Factors (SCF) for sphere of radius R and thinckness T intersected by a nozzle of radius r and thickness t at angle α. Similar diagrams can be drawn for nozzle from data in tables 1 to 4.

Table 1. Stress Concentration Factors using maximum shear stresses in spherical vessels and oblique nozzle at $\alpha = 22.5^{\circ}$

r/R	R/T	t/T=1	t/T=0.5	t/T=0.25
	50			3.25(5.84)
	100		3.09(5.81)	4.11(8.08)
1/20	200	3.69(3.97)		
	400	5.01(5.36)	5.2(11.56)	7.08(17.77)
	625	6.17(6.58)	6.22(14.54)	8.38(22.61)
	25			3.96(6.57)
	50		3.74(6.85)	5.0(9.42)
1/10	100	4.43(4.67)	4.78(9.64)	6.45(13.95)
	400	8.48(8.73)	8.23(19.20)	10.91(29.2)
	625	10.5(10.68)	9.88(23.77)	12.97(35.94)
	25		4.57(7.98)	6.08(10.67)
	50	5.26(5.49)	5.84(11.23)	7.81(15.84)
1/5	100	7.28(7.48)	7.49(15.90)	10.11(23.05)
	400	14.27(14.36)	14.28(31.33)	17.51(46.35)
	625	17.73(17.63)	17.9(38.53)	21.34(56,18)
	25	6.86(7.12)	7.88(14.43)	10.62(19.62)
	50	9.68(9.76)	10.3(20.57)	13.92(29.04)
1/2	100	13.54(13.61)	14.4(29.07)	18.53(42.27)
	400	26.65(26.35)	28.82(57.38)	34.13(84.39)
	625	33.1(32.41)	36.11(70.50)	41.71(97.27)

Table 2. Stress Concentration Factors using maximum principal stresses in spherical vessels and oblique nozzle at $\alpha = 22.5^{\circ}$

r/R	R/T	t/T=1	t/T=0.5	t/T=0.25
	50			3.25(5.28)
	100		3.09(4.79)	4.11(7.33)
1/20	200	3.01(2.97)		
	400	4.01(3.91)	5.19(10.69)	7.05(17.43)
	625	4.88(4.73)	6.21(13.37)	8.39(21.50)
	25			3.94(6.35)
	50		3.73(6.06)	5.02(9.45)
1/10	100	3.51(3.45)	4.77(8.98)	6.45(14.17)
	400	6.63(6.26)	8.23(17.74)	10.91(27.15)
	625	8.02(7.68)	9.89(21.19)	12.97(31.94)
	25		4.57(7.38)	6.08(10.96)
	50	4.28(4.09)	5.84(10.67)	7.81(16.16)
1/5	100	5.89(5.46)	7.49(15.26)	10.11(23.24)
	400	11.06(10.15)	13.35(28.12)	17.51(40.60)
	625	13.44(12.58)	16.23(33.25)	21.34(46.85)
	25	5.93(5.59)	7.88(14.18)	10.62(20.75)
	50	8.10(7.65)	10.3(20.03)	13.92(29.61)
1/2	100	11.26(10.37)	13.70(28.0)	18.53(40.24)
	400	21.14(18.87)	25.41(48.99)	34.13(68.59)
	625	27.78(23.28)	31.22(57.26)	41.71(78.30)

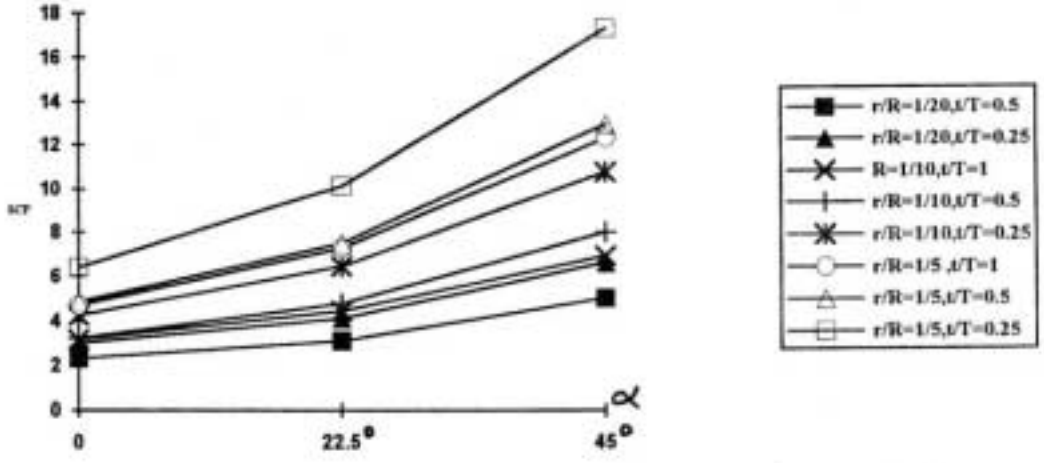

Figure 4. Variation of Stress Concentration Factors (SCF) in sphere with angle of nozzle α.

Table 3. Stress Concentration Factors using maximum shear stresses in spherical vessels and oblique nozzle at $\alpha=45^{\circ}$.

r/R	R/T	t/T=1	t/T=0.5	t/T=0.25
	50			4.9(8.53)
	100		5.03(9.42)	6.62(12.42)
1/20	200	5.51(6.72)	6.68(13.69)	9.02(17.18)
	400	7.91(9.28)	8.92(20.02)	12.77(29.55)
	25			5.98(10.0)
	50		6.05(11.17)	8.02(14.73)
1/10	100	6.93(7.94)	8.0(16.16)	10.75(22.38)
	200	9.93(10.93)	10.55(23.26)	14.18(33.55)
	400	14.2(15.09)	14.05(33.02)	18.7(48.64)
	25		7.38(13.35)	9.76(17.94)
	50	8.63(9.49)	9.73(19.08)	13.05(26.07)
1.5	100	12.29(13.08)	12.92(27.51)	17.30(38.86)
	200	17.51(18.16)	17.27(38.92)	
	400	24.69(25.13)	23.28(54.50)	30.48(78.96)

Table 4. Stress Concentration Factors using maximum principal stresses in spherical vessels and oblique nozzle at $\alpha=45^{\circ}$.

r/R	R/T	t/T=1	t/T=0.5	t/T=0.25
	50			4.9(8.0)
	100		5.03(8.07)	6.62(12.54)
1/20	200	5.0(4.74)	6.68(12.68)	9.02(18.91)
	400	7.13(6.94)	8.92(19.24)	12.17(28.04)
	25			5.98(9.91)
	50		6.05(9.70)	8.02(14.80)
1/10	100	6.12(5.66)	8.0(14.64)	10.74(22.50)
	200	8.61(8.16)	10.55(21.93)	14.18(32.60)
	400	11.83(11.29)	14.05(29.84)	18.97(44.37)
	25		7.37(12.01)	9.76(17.94)
	50	7.41(6.48)	9.72(17.56)	13.05(26.63)
1.5	100	10.44(9.12)	12.91(25.65)	17.30(38.96)
	200	14.54(12.76)	17.27(36.22)	
	400	19.79(17.58)	23.28(48.48)	30.48(69.26)

Notes:
In tables of stress concentration foctors numbers in brackets belong to the nozzles.
R is the radius and T is the thickness of the sphere.
r is the radius and t is the thinckness of the nozzle.

vessel with an oblique nozzle at 22.5° under axial and moment loading are shown in Figure 5. In this figure σ_θ and σ_ϕ are hoop and meridional stresses respectively. To calculate dimensionless values of stresses, the expression $(F/(2\pi rT))\sqrt{(R/T)}$ is used for axial load and $(M/(\pi r^2 T))\sqrt{(R/T)}$ is used for moment load. F and M are axial force and in plane bending moment on the nozzle. From the figure it is seen that the stress concentration factors at the acute side and in the nozzle are higher than those in the vessel. Nevertheless, such loadings on the nozzle need more theoretical and experimental study. Comparison between the stress concentration factors obtained from FEM and those existed in [13] and [14] is shown below. Numbers in the brackets belong to nozzle:

	from FEM	from [13]	from [14]
Axial loading on the nozzle	1.74(3.69)	1.67	1.67
Moment loading on the nozzle	1.28(3.57)	1.22	1.22
Internal pressure	4.76(8.56)	3.5	3.5

Experimental verification

It is difficult to obtain experimental data at points very close to the junction. In [3] an aluminium spherical vessel with a nozzle at 22.5° is tested under internal pressure and elastic strains are measured by strain gauges on inside and outside surfaces of the vessel and nozzle. The strains obtained from FEM are compared with experimental strains in Figure 6. In this figure ε_θ and ε_ϕ are theoretical hoop and meridional strains respectively, and $\varepsilon_{\theta e}$ and $\varepsilon_{\phi e}$ are experimental strains. As it is seen from this figure the magnitude and direction of changes of theoretical strains are in good agreement with those of the experiment except for meridional strains on the outside surface of the vessel. It is not possible to comment on the strains at points very close to the junction but theoretical strains may be evaluated higher than their

Table 5. Variation of SCF values for sphere against α. Data are not available for r/R=1/20, t/T=1.

R/T=100	r/R=1/20			r/R=1/10			r/R=1/5		
t/T α	1	0.5	0.25	1	0.5	0.25	1	0.5	0.25
0°	----	2.3	2.98	3.15	3.2	4.25	4.68	4.86	6.39
22.5°	----	3.09	4.11	4.43	4.78	6.45	7.28	7.49	10.11
45°	----	5.03	6.62	6.93	8.0	10.75	12.29	12.92	17.30

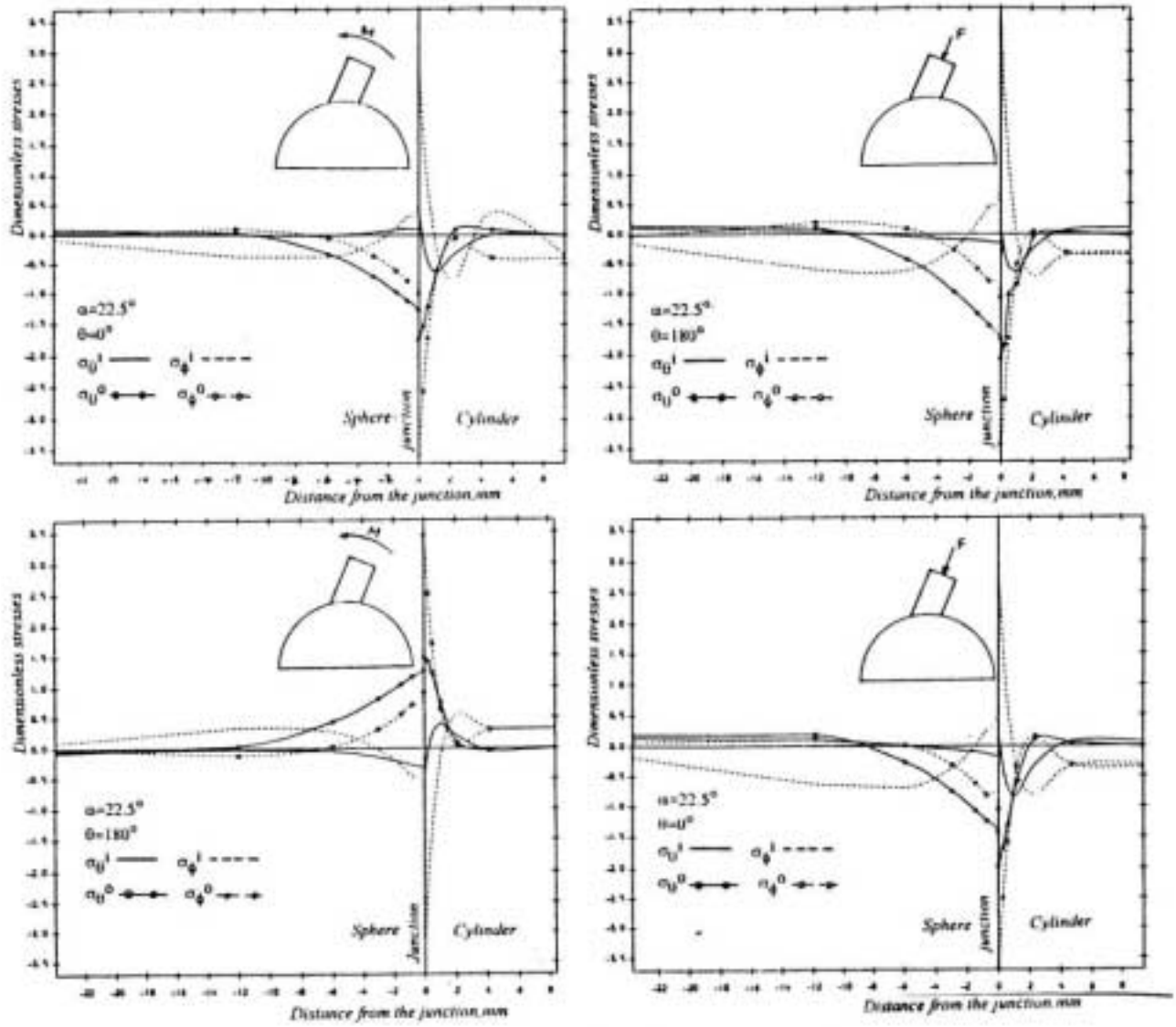

Figure 5. FEM dimensionless stresses on the outer surfaces of the Model 1 under axial force F=10 N (right) and in plane bending moment M=4.66 N.m. (left)

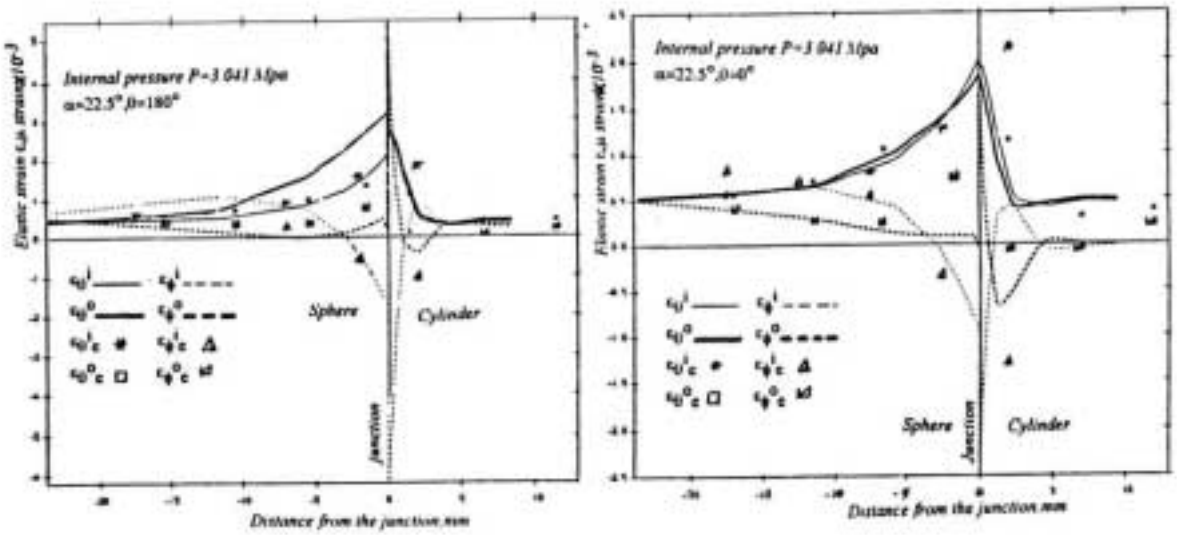

Figure 6. FEM elastic strains ε_θ and ε_ϕ on the inner and outer surfaces (superscripts i and o respectively) of Model 1. Some experimental data $\varepsilon_{\theta e}$ and $\varepsilon_{\phi e}$ are also indicated for comparison.

TABLE 6. Comparison between SCF values for sphere obtained by FEM and the values obtained by Equivalent Radius Method (numbers in brackets).

α	22.5°		45°	
ρ t/T	1	2	1	2
1	4.4(3.6)	7.3(5.4)	7.0(5.6)	12.3(8.3)
0.5	4.7(3.6)	7.4(5.6)	8.0(5.9)	12.9(8.8)
0.25	6.45(4.8)	10.1(7.3)	10.8(7.9)	17.4(11.5)

real magnitudes.

DISCUSSION

From Figure 2 it is observed that the membrane state of stress in a vessel with a nozzle at 45° appears at a distance from the junction which is approximately three times that of radial nozzle. This is an indication of very high stresses in such connections. Due to geometrical discontinuity in the structure, abrupt changes in stress and strain field are quite visible.

Diagrams of SCF versus $\sqrt{(R/T)}$ indicate linear relation between these quantities. This fact can be used to determine SCF values by linear interpolation whenever necessary and thus to reduce the number of models that must be studied.

Figure 4 shows that the slope of the SCF curves for small values of α is not very steep but for angles larger than 22.5° the slope is considerable. This subject is not considered in [5]. Regarding r/R ratio, the SCF values increase with α gently up to 22.5° for lower values of r/R. For higher values of r/R the increase in SCF is more rapid. This conclusion can not be drawn from data presented in [4] because SCF values are under estimated.

By investigating the factors in Table 6, it is observed that the SCF values calculated by the so called equivalent radius method are generally lower than the values obtained by FEM. Only for values of $\rho=(r/R)\sqrt{(R/T)}\leq 1$ and $30\leq R/T\leq 150$, the factors obtained by two methods are close to each other but for $\rho\geq 2$ the differences are not negligible.

In order to obtain more accurate results in addition to the use of three dimensional elements, it is necessary to increase the number of elements on the acute side of the connection. The variation of stresses with circumferential variable θ in this region is very severe

and the elements may not be considered thin because their sides are small compared to their thickness.

Figure 5 shows that maximum stresses under external loadings appear in the nozzle. Although, the stress distribution patterns on acute and obtuse sides are different, for axial load this difference is not significant. Investigation of Tressca stress contours for moment loading on the nozzle shows that at a region within $\theta = 90^\circ$ a substantial increase in stress field appears which needs to be investigated. Nevertheless in external loadings, the maximum stress concentration factors appear on the outside surface of the acute side of the nozzle. For external loading, the stress concentration factors in the nozzle are higher than those in the vessel as it is the case under internal pressure loading.

CONCLUSION

Finite element method and general shell element of ABAQUS computer program can be used to analyze nonsymmetric structure of sphere-cylinder because of simplicity and speed. Care should be taken that the stress concentration factors of the structure may be over estimated in comparison to their actual values. Presence of fillet radius at junction is an effective means for keeping the stress concentration factors down.

The dimensionless parameter $\rho = (r/R)\sqrt{(R/T)}$ which is normally used in previous works for plotting SCF values is not suitable. We suggest that the parameter $\sqrt{(R/T)}$ be used instead. If this parameter is used to draw the SCF diagrams, they will appear linear apart from some small deviations. Hence linear interpolation of values is permissible. It must be noticed that the higher values of SCF appear in the nozzle. The increase in SCF values with α, specially for $\alpha > 22.5^\circ$, is significant and must be taken into account.

The use of experimental method and rules like "equivalent radius method" is not sufficient for analyzing the structure. Present study shows that research programs must be launched in order to improve these methods and rules which are used in oblique nozzle design under internal pressure. If the nozzle is under external loadings, more studies should be done.

LIST OF SYMBOLS

R	Mean radius of sphere
T	Thickness of sphere
r	Mean radius of cylinder
t	Thickness of cylinder
α	Angle of obliquity
ρ	Dimensionless parameter
P	Internal pressure
F	Axial force on the nozzle
M	Moment load on the nozzle
σ_1, σ_2	Principal stresses
σ_θ	Hoop stress
σ_ϕ	Meridional stress
τ_{max}	Maximum shear stress
$\varepsilon_\theta e$	Experimental hoop strain
$\varepsilon_\phi e$	Experimental meridional strain
ε_θ	Theoretical hoop strain
ε_ϕ	Theoretical meridional strain
SCF	Stress concentration factor
E	Modulus of elsticity
v	Poisson's ratio
θ	Circumferentcial angle

ACKNOWLEDGEMENT

Many thanks are due to the Ministry of Culture and Higher Education of Iran for its support and to The University of Manchester Regional Computer Centre (UMRCC) for providing the facilities to do the research. I would like to thank Dr. M. Robinson and professor R. Kitching for their helps and guidance.

REFERENCES

1. *ASME Boiler and Pressure Vessel Code*, Section III-Division 1, (1986) edition.
2. *British Standard 5500*, Issue 2, August (1988).
3. K. Naderan-Tahan, "Stress Analysis of Spherical Shells with one and/or two Neighbouring Nozzles Under Internal Pressure and External Loading by Finite Element Method. A Parametric Survey" Ph. D. Thesis, (1989).
4. F. A. Lecki, D. J. Payn and R. K. Penny, "Elliptical Discontinuities in Spherical Shells", *Journal of Strain Analysis*. Vol 2 No 1, (1967), pp. 34-42.
5. D. E. Johnson, "Stresses in a Spherical Shell with a Non Radial Nozzle", *Journal of Applied Mechanics, June* (1967), pp. 299-307.
6. J. C. Yu, C. H. Shaw and W. A. Shaw, "Stress Distribution of a Cylindrical Shell Non Radially Attached to a Spherical Pressure Vessel" Pressure Vessel and Piping Conference, San Francisco California *ASME Paper* No 71-PVP-42, May 10-12, (1972).
7. J. C. Yu, W. A. Shaw and C. H. Chen, "Stress Distribution of Cylindrical Shell Non Radially Penetrated into a Spherical Pressure Vessel", in Proceedings Second International Conference on Pressure Vessel Technology, Part 1: Design and Analysis, *ASME*, New York, (1973), pp. 115-128.
8. R. C. Gwaltney and W. L. Greenstreet, "Comparison of Theoretical and Experimental Stresses for Spherical Shells Having Single Non Radial Nozzles", Pressure Vessel Technology Part 1: Design and Analysis, Second International conference, (1973), pp. 85-103.
9. M. M. Levin, "Photoelastic Determination of the Stresses at Oblique Openings in Plates and Shells", *WRC Bulletin* 153, August (1970) pp. 67-80.
10. J. L. Mershon, "Interpretive Report on Oblique Nozzle Connection in Pressure Vessel Heads and Shells under Internal Pressure Loadings", *WRC Bulletin* 153, August (1970) pp. 1-31.
11. ABAQUS, Hibbit, Karlson and Sorenson, Inc., 35, South Angel Street, Providence, 02906, (1984) ed.
12. K. Naderan-Tahan, "Stress Concentration Factors in Spherical Vessels with Single Radial Nozzle by Finite Element Method-a Parametrci Survey", Mechanical Engineering Dept., Shahid Chamran University, Ahwaz, Iran.
13. F. A. Leckie and R. K. Penny, "Stress Concentration Factors for the stresses at Nozzle intersections in Pressure Vessels", *WRC Bulletin 90*, September (1963).
14. Rudy Bechman, "Stress Concentration Factors in Spheres with Radial Flush Nozzles", CRIF-MT129, Center de Recherches Scientifiques et Techniques del Industrie des Fabrications Metaliques, Feb. (1979).